

Electronic Supplementary Information (ESI):

**Precursor-mediated synthesis and sensing properties of wurtzite ZnO
microspheres composed of radially aligned porous nanorods**

Jun Zhao,^a Xiaoxin Zou,^{a,b,*} Li-Jing Zhou,^a Liang-Liang Feng,^a Pan-Pan Jin,^a Yi-Pu Liu^a and Guo-Dong Li^{a,*}

^a State Key Laboratory of Inorganic Synthesis and Preparative Chemistry, Jilin University,
Changchun 130012, P.R. China

^b Department of Chemistry and Chemical Biology, Rutgers, The State University of New Jersey, NJ
08854, USA.

* E-mail: G. D. Li, lgd@jlu.edu.cn;

X. X. Zou, chemistryzouxx@gmail.com

Experimental section

Materials: Zinc acetate dihydrate, ethanol, isopropanol were purchased from Beijing Chemical Factory. Glycerol was purchased from Sinopharm Chemical Reagent Co., Ltd. The reference ZnO sample was purchased from Tianjin Jinfeng Chemical Industry Co., Ltd. All the above chemicals were used without further purification and deionized water was used in all experiments.

Synthesis of ZMG-1 and ZnO-1: For the synthesis of ZMG-1, $\text{Zn}(\text{CH}_3\text{COO})_2 \cdot 2\text{H}_2\text{O}$ (0.30 g) and glycerol (13 mL) were added into isopropanol (40 mL). The resulting solution was transferred into a 60 mL Teflon-Lined autoclave, which was treated at 85 °C for 2 h. After cooling to room temperature, the white precipitate was washed several times with deionized water and ethanol, and dried in an oven overnight at 80 °C in air. The obtained solid product was labeled as ZMG-1. The ZnO-1 material was obtained by calcining the ZMG-1 in a muffle furnace at 450 °C for 2 h.

Synthesis of ZMG-2: For the synthesis of ZMG-2, $\text{Zn}(\text{CH}_3\text{COO})_2 \cdot 2\text{H}_2\text{O}$, (0.30 g) was added into pure glycerol (53 mL) and stirred at room temperature. After stirring for 10 min, the mixture was transferred into Teflon-lined autoclave, which was treated at 160 °C for 2 h. After cooling to room temperature, the white precipitate (ZMG-2) was washed several times with deionized water and ethanol, and dried in an oven overnight at 80 °C in air.

General Characterization: The powder X-ray diffraction (XRD) patterns were recorded on a Rigaku D/Max 2550 X-ray diffractometer using CuK α radiation ($\lambda = 1.5418 \text{ \AA}$) operated at 200 mA and 50 kV. The scanning electron microscopic (SEM) images were taken on a JEOL JSM 6700F electron microscope. The transmission electron microscopy (TEM) and high-resolution TEM (HRTEM) images were obtained on a Philips-FEI Tecnai G2S-Twin with a field emission gun operating at 200 kv. The Brunauer-Emmett-Teller surface areas and Nitrogen adsorption-desorption isotherms of the samples were measured by using a Micromeritics ASAP 2020M system. The infrared (IR) spectra were recorded on a Bruker IFS 66V/S FTIR spectrometer using KBr pellets. The thermal gravimetric analysis curve was recorded on a NETZSCH STA 449C TG thermal analyzer from 25 to 800 °C at a heating rate of 10 °C min⁻¹ in air. The X-ray photoelectron spectroscopy (XPS) was performed on an ESCALAB 250 X-ray photoelectron spectrometer with a monochromated X-ray source (Al KR $h\nu = 1486.6 \text{ eV}$).

Sensor Fabrication and Testing: The gas sensor was fabricated by pasting a viscous slurry of the obtained samples mixed with deionized water in a weight ratio of 100:25 onto an alumina tube with a diameter of 1 mm and a length of 4 mm, which was positioned with a pair of Au electrodes and four Pt wires on both ends of the tube. A Ni-Cr wire was used as a heater, controlled by varying voltage, ensured both substrate heating and operating temperature control. For comparison, all of the sensors were fabricated using same method, and only difference may be the ZnO material. Gas sensing tests were performed on a commercial CGS-8 Gas Sensing Measurement System (Beijing Elite Tech Company Limited). In the system, a load resistor was connected in series with the sensor, and Fig. S14 shows the working principle of this system. The resistance (or output voltage, V_{out}) of a sensor in air or a target gas was measured by monitoring the terminal voltage of the load resistor at a test circuit voltage of 5 V (V_c).

Gas sensing properties were measured using a static test system which included a test chamber (~ 1 L in volume) at room temperature (~ 25 °C). Environmental air with a relative humidity of ~20 % was used as both a reference gas and a diluting gas to obtain the desired concentrations of target gases. A typical testing procedure was as follows. After the target gas was injected into the test chamber for about 10 min by a syringe, the sensor was put into the test chamber. When the response reached a constant value, the sensor was taken out to recover in fresh air. The sensor sensitivity is defined as the ratio R_a/R_g , where R_a and R_g are the electrical resistance of the sensor in atmospheric air and in the testing gas, respectively.

The gas sensing behavior of ZnO is generally ascribed to the interaction of surface chemisorbed oxygen and the gas molecules to be detected.^[S1] The oxygen molecules in air are chemisorbed on the ZnO surface and function as electron acceptors. The chemisorbed oxygen extracts electrons from the conduction band of ZnO, leading to the creation of a potential barrier and thus a high resistance state. When the sensor is exposed to a reductive gas (such as ethanol) at moderate temperature, the gas reacts with the surface oxygen species, resulting in a decrease of the amount of adsorbed oxygen. As a consequence, the height of the potential barrier is reduced, and the resistance of the whole sensing layer decreases significantly.

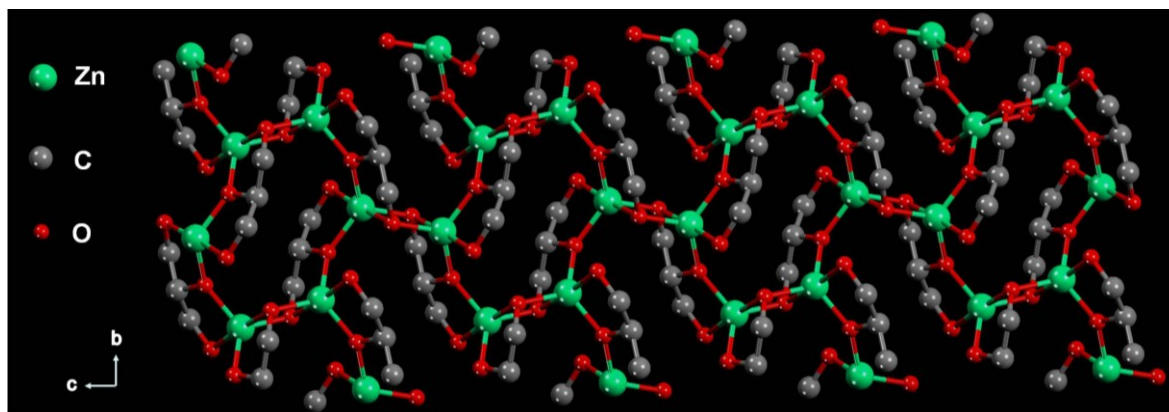


Fig. S1 The crystal structure of zinc monoglycerolate.^[S2]

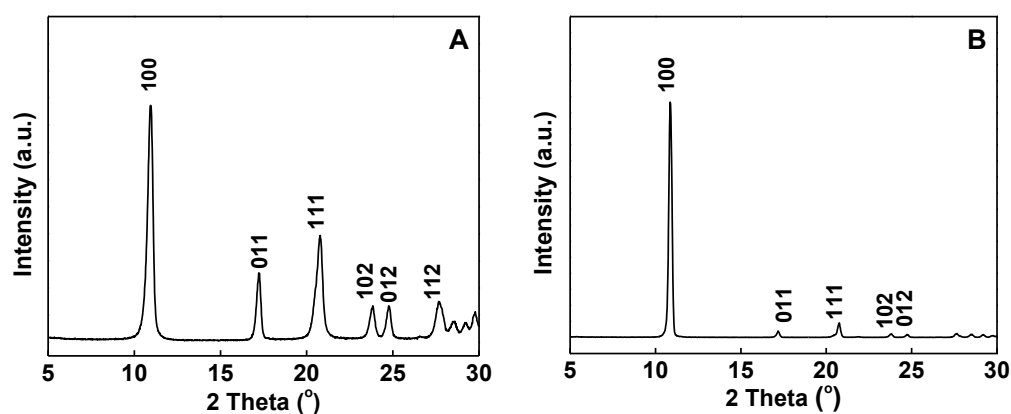


Fig. S2 XRD patterns of (A) ZMG-1 and (B) ZMG-2.

As shown in Fig. S2, ZMG-1 and ZMG-2 show similar XRD patterns, which are indexed as zinc monoglycerolate (JCPDS card No. 23-1975).^[S1] Although isopropanol as a solvent was introduced deliberately into the reaction system, the crystal structure of zinc monoglycerolate did not change at this condition. However, isopropanol may prefer to be adsorbed on the (100) crystal surface of zinc monoglycerolate particles in the case of ZMG-1, and thereby inhibits its further growth, as indicated by the obvious decreased ratio of (100)/(011) for ZMG-1 compared to that of ZMG-2 (Fig. S2). This may be one of the reasons why isopropanol can efficiently control the growth of zinc monoglycerolate, resulting in the formation of a hierarchical structure (ZMG-1), instead of large plate-like particles (ZMG-2).

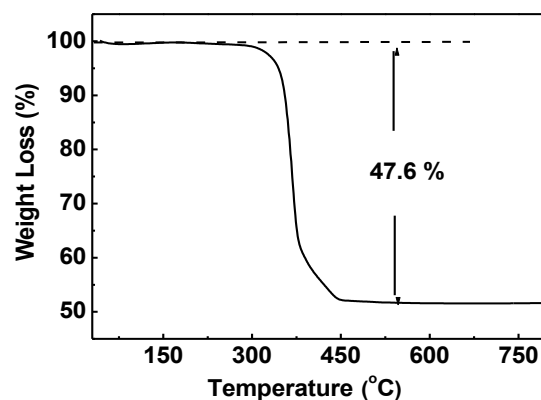


Fig. S3 TG curve measured in air for ZMG-1. TG analysis of ZMG-1 was carried out in air from 25 to 800 °C. The ZMG-1 decomposed in the range of 300 ~ 450 °C. According to TG analysis, it is estimated that the empirical composition of ZMG-1 is $C_3H_6O_3Zn$, which is in agreement with the previously-reported result. ^[S1]

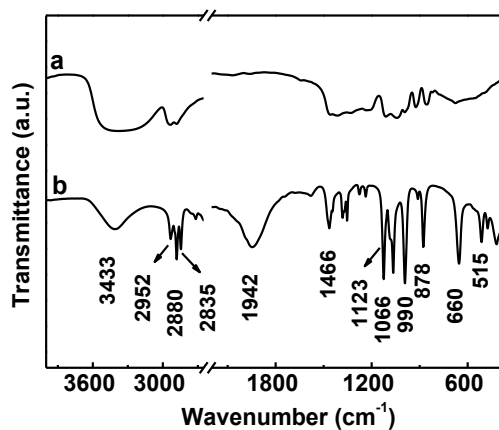


Fig. S4 IR spectra of (a) glycerol and (b) ZMG-1. Compared to that of glycerol, the narrowing of the glycerol bands in ZMG-1 is due to the crystalline nature of this material. The bands at 1066 and 1123 cm^{-1} are assigned to the stretching mode of alcoholic C-O. The bands at 1466 cm^{-1} and 3433 cm^{-1} are assigned to the bending mode and stretching mode of -OH, respectively. The absorption bands below 660 cm^{-1} are attributed to the Zn-O stretching vibration, which indicates the presence of Zn-O bond in the sample.

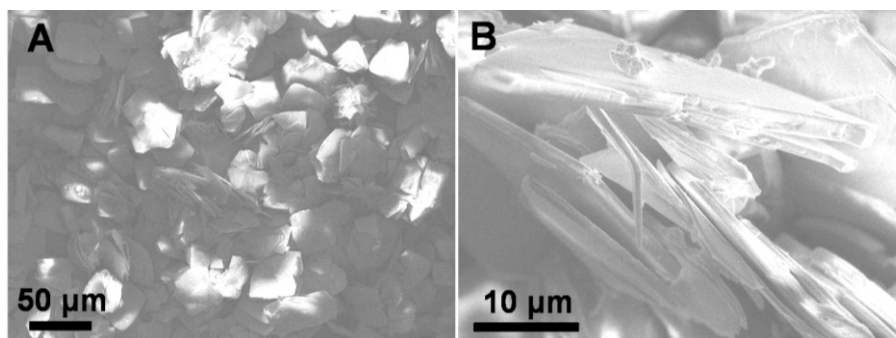


Fig. S5 SEM images of ZMG-2. It is seen that ZMG-2 contains large plate-like microcrystals.

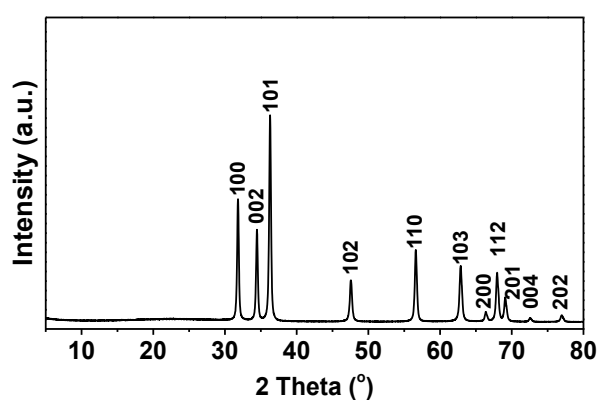


Fig. S6 XRD pattern of ZnO-1. It is clear that the XRD pattern related to ZMG-1 (Fig. S2A, ESI†) completely disappeared. It is believed that after thermal treatment, zinc monoglycerolate (ZMG-1) was completely converted into zinc oxide (ZnO-1).

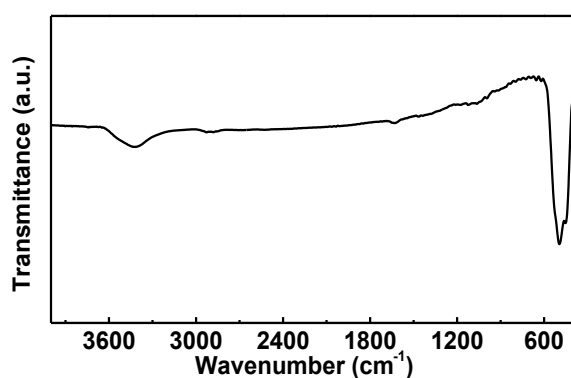


Fig. S7 IR spectrum of ZnO-1. Comparison of the IR spectra of ZnO-1 and ZMG-1 (Fig. S4b) revealed that the total disappearance of the absorption peaks related to glycerol molecules in ZMG-1, demonstrating the complete thermal conversion of the ZMG-1 precursor to the ZnO material.

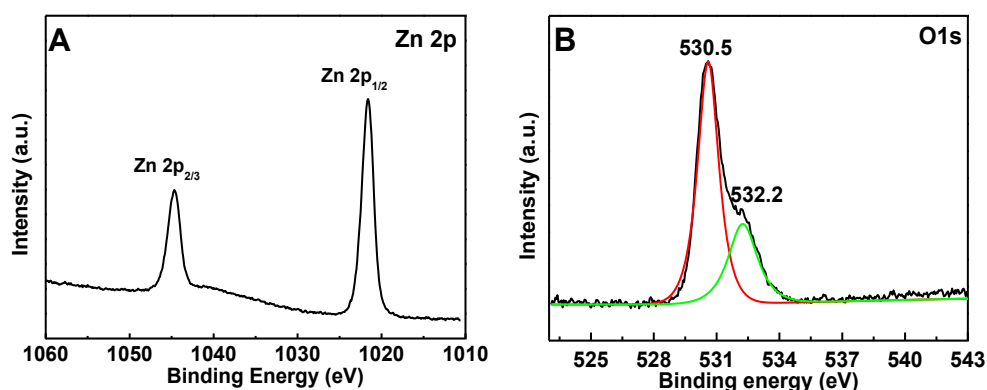


Fig. S8 (A) Zn 2p and (B) O1s XPS spectra of ZnO-1. It is seen that the Zn2p spectrum for ZnO-1 (Fig. S8A) exhibits two peaks at 1021.5 and 1044.7 eV, which are assigned to the 2p_{1/2} and 2p_{3/2} core level of Zn²⁺ in ZnO, respectively.^[S3-5] In the Fig. S8B, the fitting for the O1s peak reveals the presence of a major peak at 530.5 eV with a shoulder at 532.2 eV. The primary peak at 530.5 eV for ZnO-1 is attributable to Zn-O-Zn oxygen.^[S3-5] The shoulder peak at 532.2 eV is associated with the presence of loosely bound oxygen, such as absorbed O₂ and water.^[S3-5]

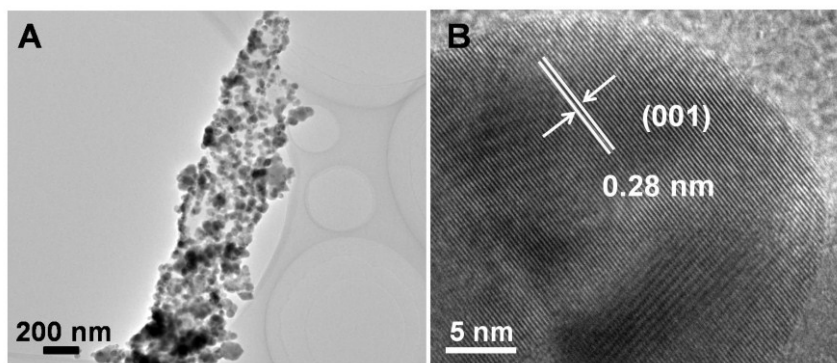


Fig. S9 (A) TEM and (B) HRTEM images of ZnO-1. The TEM image of ZnO-1 (Fig. S9A) shows that this material is composed of randomly but spatially interconnected nanocrystals of 20-30 nm in size. In the HRTEM image (Fig. S9B), the observed lattice spacing is about 0.28 nm, which corresponds to the interplanar distance of the (100) plane of wurtzite ZnO.

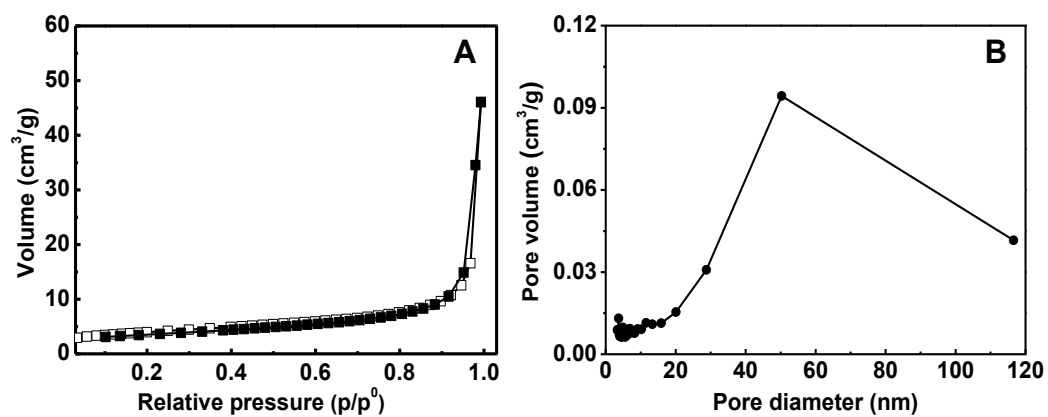


Fig. S10 (A) N₂ adsorption-desorption isotherms and (B) the corresponding pore size distribution of ZnO-1.

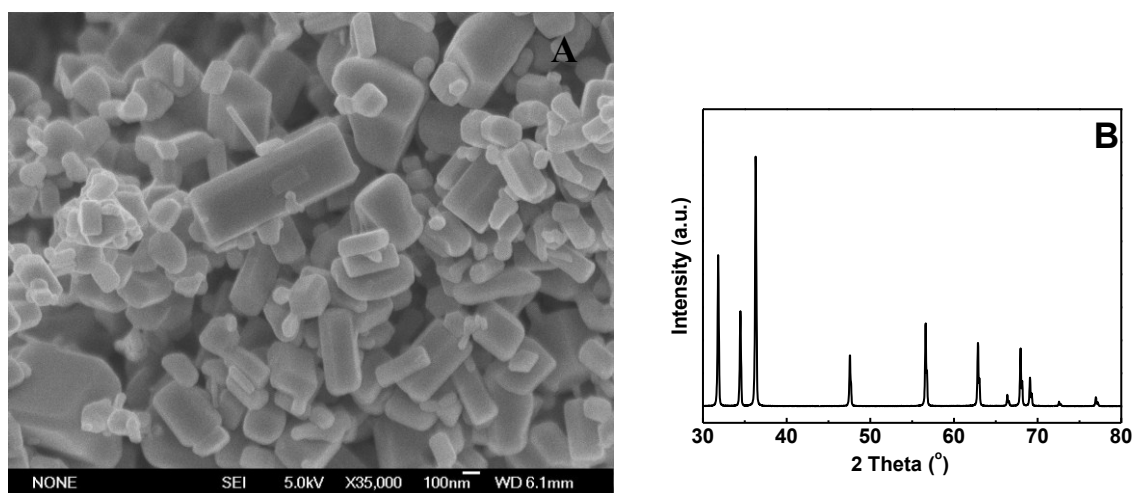


Fig. S11 (A) SEM image and (B) XRD pattern of Com-ZnO. The SEM image of Com-ZnO shows that this material is composed of ZnO nanoparticles with an inhomogeneous diameter distribution of 30-200 nm. The XRD pattern of Com-ZnO confirms that this material is made of pure wurtzite ZnO.

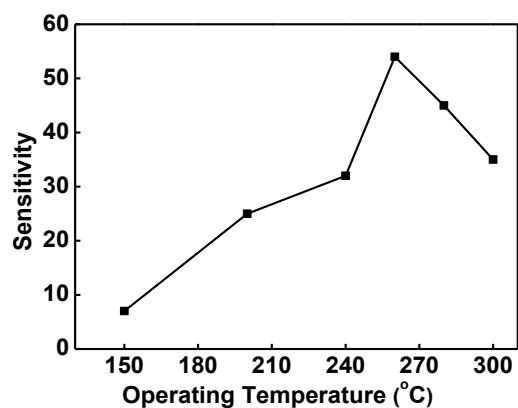


Fig. S12 Sensitivity of the ZnO-1 sensor varied against the operating temperature for the detection of ethanol with a concentration of 100 ppm. As revealed in the Fig. S12, the ZnO-1 sensor shows the highest sensitivity toward ethanol at 260 °C.

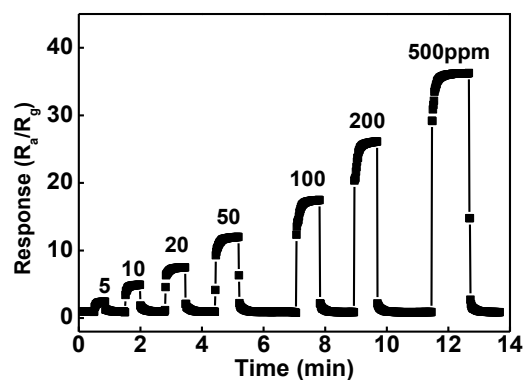


Fig. S13 Dynamic response–recovery curve of the sensor based on Com-ZnO for ethanol detection.

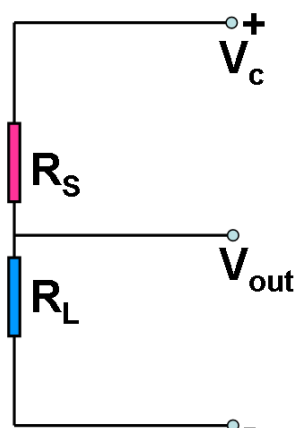


Fig. S14 A schematic diagram of the measurement circuit. R_L : load resistance; R_s : sensor resistance; V_c : operating circuit voltage; V_{out} : output voltage.^[S6,7]

Table S1 Viscosity of glycerol and isopropanol.^[S8]

| Substance | Viscosity $\text{mN} \cdot \text{s} \cdot \text{m}^{-2}$ |
|-------------|---|
| Glycerol | 934 |
| Isopropanol | 1.765 |

ESI references:

- [S1] M. E. Franke, T. J. Koplín and U. Simon, *Small*, 2006, **2**, 36.
- [S2] T. W. Hambley, M. R. Snow, *Aust. J. Chem.*, 1983, **36**, 1249.
- [S3] E. D. Rosa, S. Sepulveda-Guzman, B. Reeja-Jayan, A. Torres, P. Salas, N. Elizondo, M. J. Yacaman, *J. Phys. Chem. C*, 2007, **111**, 8489.
- [S4] X. Wang, K. Huo, F. Zhang, Z. Hu, P. K. Chu, H. Tao, Q. Wu, Y. Hu, J. Zhu, *J. Phys. Chem. C*, 2009, **113**, 170.
- [S5] N. S. Ramgir, D. J. Late, A. B. Bhise, M. A. More, I. S. Mulla, D. S. Joag, K. Vijayamohanan, *J. Phys. Chem. B*, 2006, **110**, 18236.
- [S6] X. Liu, J. Zhang, L. Wang, T. Yang, X. Guo, S. Wu, S. Wang, *J. Mater. Chem.*, 2011, **21**, 349.
- [S7] J. Su, X.-X. Zou, Y.-C. Zou, G.-D. Li, P.-P. Wang, J.-S. Chen, *Inorg. Chem.*, 2013, **52**, 5924.
- [S8] J. Zhao, X. X. Zou, J. Su, P. P. Wang, L. J. Zhou and G. D. Li, *Dalton Trans.*, 2013, **42**, 4365.